Centrum voor Wiskunde en Informatica

**REPORT***RAPPORT*

Splitting methods for partial Volterra integro-differential equations

H. Brunner, P.J. van der Houwen, B.P. Sommeijer

Modelling, Analysis and Simulation (MAS)

**MAS-R9909 April 1999**

Report MAS-R9909
ISSN 1386-3703

CWI
P.O. Box 94079
1090 GB Amsterdam
The Netherlands

# Splitting Methods for Partial Volterra Integro-Differential Equations

H. Brunner
*Memorial University of Newfoundland, Department of Mathematics and Statistics*
*St. John's, NF, Canada A1C 5S7*

P.J. van der Houwen & B.P. Sommeijer
*CWI*
*P.O. Box 94079, 1090 GB Amsterdam, The Netherlands*

ABSTRACT
The spatial discretization of initial-boundary-value problems for (nonlinear) parabolic or hyperbolic PDEs with memory terms leads to (large) systems of Volterra integro-differential equations (VIDEs). In this paper we study the efficient numerical solution of such systems by methods based on linear multistep formulas, using special factorization (or splitting) techniques in the iterative solution of the resulting (expensive) nonlinear algebraic equations. The analysis of the convergence and stability properties is complemented by numerical examples.

*1991 Mathematics Subject Classification:* 65L06, 65R20
*Keywords and Phrases:* numerical analysis, Volterra integral equations, splitting methods, stability.
*Note:* Work carried out under project MAS 1.4 - 'Exploratory Research' .

## 1. Introduction

We consider efficient time integration methods for the spatially semidiscretized initial-boundary-value problem for the partial Volterra integro-differential equation (PVIDE) of the generic form

$$(1.1)\qquad \frac{\partial u(t,\mathbf{x})}{\partial t} = L\big(t, \mathbf{x}, u(t,\mathbf{x}), v(t,\mathbf{x})\big), \quad v(t,\mathbf{x}) := \int_c^t k\big(t, \tau, u(t,\mathbf{x}), u(\tau,\mathbf{x})\big)\, d\tau,$$

with appropriate boundary conditions on the boundary $\partial\Omega$ of the spatial domain $\Omega$ in $\mathbb{R}^d$. Here, L is a differential operator in the space variable $\mathbf{x} \in \Omega$ (with $\Omega$ bounded), $t \geq t_0$, $c \leq t_0$, and k is a given real function. If the lower limit c in the integral operator is less than the initial point $t_0$, then it will be assumed that the "history" of $u(t,\mathbf{x})$ is known for $c \leq t \leq t_0$ and $\mathbf{x} \in \Omega$. Such problems, or closely related ones (e.g. PVIDEs with constant delays) occur more and more frequently in the mathematical modelling of physical or biological phenomena where memory effects play a non-negligible role. Due to a better understanding of the analytical theory of PVIDEs such models are becoming increasingly complex, and there is a distinct need for efficient numerical methods to solve these equations. Since, as Volterra [21] (who introduced partial integro-differential equations and coined the name "equazioni integro-differenziali" in this paper) already pointed out, "*the problem of solving integro-differential equations constitutes in general a problem that is fundamentally different from the one of solving differential equations* ...", these numerical methods have to be able to cope with these problems.

We present four representative examples of PVIDEs arising in applications; for additional details and other PVIDE models the reader is referred to [1, 4, 5, 10, 11, 13, 14, 15, 16, 18, 19, 20, 22, 23, 24, 25] and the references listed in these papers and books.

**Example 1.1.** Nonlinear conservation law with memory [6]. This model problem was motivated by the more complex physical problem of the extension of a finite, homogeneous, elastoviscous body moving under the action of an assigned body force g (see [6]); it is given by

$$(1.2) \qquad \frac{\partial u(t,x)}{\partial t} = -\frac{\partial \phi(u(t,x))}{\partial x} - \int_{-\infty}^{t} \kappa'(t-\tau)\,\frac{\partial \psi(u(\tau,x))}{\partial x}\,d\tau + g(t,x), \quad -\infty < t < \infty,$$

where $\phi$, $\psi$: $\mathbb{R} \to \mathbb{R}$ are given smooth constitutive functions; $\kappa$: $[0,\infty) \to \mathbb{R}$ is a given (positive, nonincreasing) memory kernel. It is assumed that the (smooth) history of the motion of the body, $u(t,x) = h(t,x)$, up to time $t = 0$ is known. Note that for $\psi \equiv 0$ and $g \equiv 0$, (1.2) reduces to the (quasilinear and hyperbolic) Burgers' equation. ♦

**Example 1.2.** The two-dimensional version of the mathematical model for the evolution of a community of species (or population) that is allowed to diffuse spatially is described by (cf. [5, p. 6 and p. 183] and [10])

$$(1.3) \qquad \frac{\partial u(t,\mathbf{x})}{\partial t} = (\Delta + b)u(t,\mathbf{x}) - \int_{t_0}^{t} \kappa(t-\tau)u(\tau,\mathbf{x})\,u(t,\mathbf{x})\,d\tau + g(t,\mathbf{x}),$$

where u is the size of the population, $\Delta$ is the two-dimensional Laplace operator, g represents external influences, the kernel $\kappa$ is given by $\kappa(t) = T^{-2}\, t\, \exp(-\,t\,T^{-1})$ or $\kappa(t) = T^{-2} \exp(-\,t\,T^{-1})$, and T is the point where the so-called "strong" generic delay kernel $\kappa(t)$ assumes its maximum. This example will be used in our experiments reported in Section 4. ♦

**Example 1.3.** A PVIDE with nonlocal convection is given by

$$(1.4) \qquad \frac{\partial u(t,x)}{\partial t} = \frac{\partial^2 u(t,x)}{\partial x^2} - \frac{\partial}{\partial x} \int_{c}^{t} \kappa(t-\tau)\,u(\tau,x)\,u(t,x)\,d\tau + \gamma u(t,x)\big(1 - u(t,x)\big),$$

where $\gamma > 0$ and $c \le 0$. The (smooth) kernel $\kappa$ describes the nonlocal density in this population model. This equation differs from the Fischer-type PVIDE studied in [14], where the quadrature term represents a convolution over the space variable.♦

**Example 1.4.** The mathematical model describing a spatially aggregated population model with (nonlinear) diffusion and (nonlocal) convection in two spatial dimensions is given by the PVIDE

$$(1.5) \qquad \frac{\partial u(t,\mathbf{x})}{\partial t} = \Delta u(t,\mathbf{x}) - (\mathbf{v}^T\nabla) \int_c^t \kappa(t-\tau)\, u(\tau,\mathbf{x})\, u(t,\mathbf{x})\, d\tau + g(t,\mathbf{x}), \quad c \le 0.$$

The main difference with equation (1.3) consists of the convection operator $\mathbf{v}^T\nabla$ in front of the integral term. Here, $\mathbf{v}^T = (v_1,v_2)$ is a given velocity vector and $\nabla$ is the two-dimensional gradient operator. As in Example 1.3, $\kappa$ is nonnegative and smooth. Equation (1.5) differs from the PVIDEs studied in [13] by the quadrature term which is here based on time convolutions, whereas [13] treats the case of space convolution. This is the second example to be used in our experiments to illustrate the use of splitting methods in solving PVIDEs. ♦

Note the "nonstandard" form of the PVIDEs in (1.3), (1.4) and (1.5) (giving rise to the kernel $k = k\big(t, \tau, u(t,\mathbf{x}), u(\tau,\mathbf{x})\big)$ in (1.1)), which is typical for mathematical models in population dynamics.

In this paper, we shall confine our considerations to PVIDEs without delay, i.e. $c = t_0$. The numerical treatment of PVIDEs with delay will be subject of future research.

The outline of the paper is as follows. Section 2 defines the linear multistep discretization of spatially discretized PVIDEs and derives stability regions along the lines of the stability analysis of Matthys [12]. Section 3 gives a stability analysis for the methods which result from the approximately factorized iteration of the modified Newton systems and presents the main results of the paper. Stability regions are derived for PVIDEs in one, two and three spatial dimensions. Finally, Section 4 reports numerical experiments for the problems (1.3) and (1.5).

## 2. Discretization

Discretization of the differential operator L in the PVIDE (1.1) on a spatial grid of gridpoints in $\Omega$ leads to an initial-value problem (IVP) for a system of VIDEs:

$$(2.1) \qquad \mathbf{y}'(t) = \mathbf{f}\big(t, \mathbf{y}(t), \mathbf{z}(t)\big), \quad \mathbf{z}(t) := \int_{t_0}^t \mathbf{k}\big(t, \tau, \mathbf{y}(t), \mathbf{y}(\tau)\big)\, d\tau, \quad \mathbf{y}(t_0) = \mathbf{y}_0,$$

where $\mathbf{f}$ represents the discretization of L and where the vector-valued quantities $\mathbf{y}$, $\mathbf{z}$ and $\mathbf{k}$ are the discrete analogues of u, v and k, that is, the number of components of $\mathbf{y}$, $\mathbf{z}$ and $\mathbf{k}$ equals the number of grid points used in the spatial discretization of L. Note that the boundary conditions associated with (1.1) are lumped into the right-hand side of (2.1).

Since $\mathbf{f}$ originates from the differential operator L, the Jacobian matrices $\partial\mathbf{f}/\partial\mathbf{y}$ and $\partial\mathbf{f}/\partial\mathbf{z}$ may possess eigenvalues of large magnitude. Let us denote the Jacobian matrices of the function $\mathbf{f}(t, \mathbf{y}, \mathbf{z})$ with respect to $\mathbf{y}$ and $\mathbf{z}$ by $\mathbf{f_y}$ and $\mathbf{f_z}$, and the Jacobian matrices of $\mathbf{k}(t, s, \mathbf{y}, \mathbf{w})$ with respect to $\mathbf{y}$ and $\mathbf{w}$ by $\mathbf{k_y}$ and $\mathbf{k_w}$. In this paper, we restrict our considerations to the case where $\mathbf{f_y}$ is much more stiff than $\mathbf{f_z}$, $\mathbf{k_y}$ and $\mathbf{k_w}$, that is, the magnitude of the eigenvalues of $\mathbf{f_y}$ is much larger than the magnitude of the eigenvalues of $\mathbf{f_z}$, $\mathbf{k_y}$ and $\mathbf{k_w}$. The spatial discretization of the PVIDES given in the Examples 1.2, 1.3 and 1.4 have these properties, because the spatial discretization of diffusion terms leads to much larger eigenvalues than the discretization of convection terms.

## 2.1. LMM discretization

By introducing the function

$$(2.2) \qquad \mathbf{z}(t,s) := \int_{t_0}^{s} \mathbf{k}\big(t, \tau, \mathbf{y}(t), \mathbf{y}(\tau)\big)\, d\tau,$$

the values of $\mathbf{z}(t)$ needed when solving $\mathbf{y}(t)$ from (2.1) can be obtained by integrating the IVP

$$(2.3) \qquad \frac{\partial \mathbf{z}(t,s)}{\partial s} = \mathbf{k}\big(t, s, \mathbf{y}(t), \mathbf{y}(s)\big), \quad \mathbf{z}(t,t_0) = \mathbf{0}$$

from $s = t_0$ until $s = t$, and by setting $\mathbf{z}(t) = \mathbf{z}(t,t)$.

We shall use a linear multistep method (LMM) for integrating the equations (2.1) and (2.3). Let the LMM be defined by the Dahlquist polynomials $\rho$ and $\sigma$. Then, we obtain for (2.1) the formula

$$(2.4) \qquad \rho(E)\mathbf{y}_n = h\sigma(E)\, \mathbf{f}\big(t_n, \mathbf{y}_n, \mathbf{z}_n\big), \quad n = 0, 1, ...,$$

where E is the forward shift operator. Likewise, applying the same LMM to (2.3) with $t = t_n$ and $\mathbf{y}(t) = \mathbf{y}_n$, i.e. the equation

$$(2.3') \qquad \frac{d\mathbf{z}(t_n,t)}{dt} = \mathbf{k}\big(t_n, t, \mathbf{y}_n, \mathbf{y}(t)\big), \quad \mathbf{z}(t_n, t_0) = \mathbf{0},$$

yields the formula

$$(2.5) \qquad \rho(E)\mathbf{z}_\nu = h\sigma(E)\, \mathbf{k}\big(t_n, t_\nu, \mathbf{y}_n, \mathbf{y}_\nu\big), \quad \nu = 0, 1, ... , n.$$

The combined method {(2.4), (2.5)} has the same order of accuracy as the underlying LMM.

## 2.2. Stability

Next, we consider the stability of {(2.4), (2.5)}. Evidently, the LMM recursion (2.5) on its own has the same stability characteristics as the LMM. For the combined method, we need to consider the stability of the coupled formulas for $\mathbf{y}_{n+k}$ and $\mathbf{z}_{n+k}$, where k is the number of steps involved in the application of the LMM. This can be done by applying {(2.4), (2.5)} to the Brunner-Lambert test equation [3]

$$\text{(2.6)} \qquad \frac{dy(t)}{dt} = \xi y(t) + z(t), \quad \frac{dz(t)}{dt} = \eta y(t),$$

where $\xi$ and $\eta$ are complex parameters. However, in order to see clearly the meaning of these parameters we prefer to look at the first-order variation of {(2.4), (2.5)}, that is, at the linear relations

$$\rho(E)\Delta\mathbf{y}_n = h\sigma(E)\left(\mathbf{f_y}\Delta\mathbf{y}_n + \mathbf{f_z}\Delta\mathbf{z}_n\right), \ \rho(E)\Delta\mathbf{z}_n = h\sigma(E)\left(\mathbf{k_y} + \mathbf{k_w}\right)\Delta\mathbf{y}_n.$$

Writing $h\mathbf{f_z}\Delta\mathbf{z}_n = \Delta\tilde{\mathbf{z}}_n$, these relations become

$$\rho(E)\Delta\mathbf{y}_n = \sigma(E)\left(h\mathbf{f_y}\Delta\mathbf{y}_n + \Delta\tilde{\mathbf{z}}_n\right), \ \rho(E)\Delta\tilde{\mathbf{z}}_n = \sigma(E)\, h^2\mathbf{f_z}\left(\mathbf{k_y} + \mathbf{k_w}\right)\Delta\mathbf{y}_n.$$

Considering the model situation where the Jacobian matrices $\mathbf{f_y}$ and $\mathbf{f_z}\left(\mathbf{k_y} + \mathbf{k_w}\right)$ share the same eigensystems, we are led to the recursions

$$\text{(2.7)} \qquad \rho(E)\Delta\mathbf{y}_n = \sigma(E)\left(h\xi\Delta\mathbf{y}_n + \Delta\tilde{\mathbf{z}}_n\right), \ \rho(E)\Delta\tilde{\mathbf{z}}_n = \sigma(E)\, h^2\eta\Delta\mathbf{y}_n.$$

The same relations are obtained when applying {(2.4), (2.5)} to (2.6), but it is now immediately clear that $\xi$ and $\eta$, respectively, represent the eigenvalues of the matrices J := $\mathbf{f_y}$ and K := $\mathbf{f_z}\left(\mathbf{k_y} + \mathbf{k_w}\right)$ at the points (t, $\mathbf{y}$, $\mathbf{z}$) = ($t_n$, $\mathbf{y}_n$, $\mathbf{z}_n$) and (t, $\tau$, $\mathbf{y}$, $\mathbf{w}$) = ($t_n$, $t_n$, $\mathbf{y}_n$, $\mathbf{y}_n$), respectively.

Let us define the stability region by the points in the $(\xi,\eta)$- space, where the characteristic equation associated with (2.7) has its roots on the unit disk. Following Matthys [12], we write $\xi = \lambda + \mu$ and $\eta = -\lambda\mu$, so that the characteristic equation can be written in the factorized form

$$\text{(2.8)} \qquad \left(\rho(\zeta) - h\lambda\sigma(\zeta)\right)\left(\rho(\zeta) - h\mu\sigma(\zeta)\right) = 0.$$

These factors have the same form as the characteristic polynomial of the underlying LMM. Hence, the roots of (2.8) are on the closed unit disk for all $\lambda$ and $\mu$ in the stability region of the LMM, so that its stability region is given by the corresponding region in the $(\xi, \eta)$ - space. Let us consider the special case where the LMM is A-stable and where $\xi$ is either real or purely imaginary. If $\mathrm{Im}(\xi) = 0$, then necessarily $\mathrm{Re}(\xi) \le 0$ and $\mathrm{Im}(\lambda) = -\mathrm{Im}(\mu)$. Hence,

$$\mathrm{Re}(\eta) = -\left(\mathrm{Re}(\lambda).\mathrm{Re}(\mu) + \mathrm{Im}^2(\mu)\right), \quad \mathrm{Im}(\eta) = \mathrm{Im}(\mu).\mathrm{Re}(\mu - \lambda),$$

so that $\mathrm{Re}(\eta) \le 0$. Thus, the stability region of the method {(2.4), (2.5)} contains the domain

(2.9a) $\{(h\xi,h^2\eta):\ \mathrm{Im}(\xi) = 0,\ \xi \le 0,\ \mathrm{Re}(\eta) \le 0\}$.

If $\mathrm{Re}(\xi) = 0$, then $\mathrm{Re}(\lambda + \mu) = 0$. Hence, $\mathrm{Re}(\lambda) = \mathrm{Re}(\mu) = 0$, so that

$$\mathrm{Re}(\eta) = \mathrm{Im}(\lambda).\mathrm{Im}(\mu), \quad \mathrm{Im}(\eta) = 0.$$

Thus, we may conclude that the stability region contains the points $(h\xi,h^2\eta)$ with $\mathrm{Re}(\xi) = \mathrm{Im}(\eta) = 0$. Finally, using the maximum modulus theorem, we may even conclude that the stability region of the method {(2.4), (2.5)} contains the domain

(2.9b) $\{(h\xi,h^2\eta):\ \mathrm{Re}(\xi) \le 0,\ \mathrm{Im}(\eta) = 0\}$.

In order to appreciate this result, we derive the stability region of the test equation (2.6). Since (2.6) is equivalent to the second-order ODE $y'' - \xi y' - \eta y = 0$, we see that we have stability if the roots of the characteristic equation $\zeta^2 - \xi\zeta - \eta = 0$ satisfy $\mathrm{Re}(\zeta) \le 0$. Again using the transformation $\{\xi = \lambda + \mu,\ \eta = -\lambda\mu\}$, it follows that the characteristic equation has the roots $\lambda$ and $\mu$, so that the test equation (2.6) is itself stable if $\mathrm{Re}(\lambda) \le 0$ and $\mathrm{Re}(\mu) \le 0$, the same conditions we found for the LMM. We summarize the above results in the following theorem:

**Theorem 2.1.** The stability region of the test equation (2.6) and of the method {(2.4), (2.5)} generated by an A-stable LMM both contain the domains (2.9a) and (2.9b).♦

Note that in the domains (2.9a) and (2.9b) either $\xi$ or $\eta$ is required to be real-valued. This implies that for stable spatial discretizations of PVIDEs, the eigenvalues of the Jacobian matrices $J = \mathbf{f_y}$ and $K = \mathbf{f_z}(\mathbf{k_y} + \mathbf{k_w})$ at the point $(t, \tau, \mathbf{y}, \mathbf{w}) = (t_n, t_n, \mathbf{y}_n, \mathbf{y}_n)$ should not be both complex.

**Example 2.1.** Let us consider the population model (1.5) on the 2-dimensional domain $\Omega = \{0 \le x_1, x_2 \le 1\}$ with homogeneous Dirichlet boundary conditions on the boundary of $\Omega$. Discretizing $\Omega$ by a grid with uniform gridsize $\Delta x$, the Laplace operator $\Delta$ and the convection operator $\mathbf{v}^T\nabla$ can be replaced by matrices D and C. The functions **f** and **k** in (2.1) can be chosen in several ways, e.g.

(2.10a) $\mathbf{f}(t, \mathbf{y}, \mathbf{z}) = D\mathbf{y} + C\mathbf{z} + \mathbf{g}(t), \quad \mathbf{k}(t, \tau, \mathbf{y}, \mathbf{w}) = -\kappa(t-\tau)\mathbf{yw},$

(2.10b) $\mathbf{f}(t, \mathbf{y}, \mathbf{z}) = D\mathbf{y} + \mathbf{z} + \mathbf{g}(t), \quad \mathbf{k}(t, \tau, \mathbf{y}, \mathbf{w}) = -\kappa(t-\tau)C\mathbf{yw},$

(2.10c) $\mathbf{f}(t, \mathbf{y}, \mathbf{z}) = D\mathbf{y} + C\mathbf{yz} + \mathbf{g}(t), \quad \mathbf{k}(t, \tau, \mathbf{y}, \mathbf{w}) = -\kappa(t-\tau)\mathbf{w},$

where $\mathbf{g}(t)$ is the discrete analogue of $g(t,\mathbf{x})$ in (1.5) and **yw**, **yz** are defined componentwise. In the case (2.10c) the matrices J and K at the point $(t, \tau, \mathbf{y}, \mathbf{w}) = (t_n, t_n, \mathbf{y}_n, \mathbf{y}_n)$ are respectively given by $J = D + C\,\mathrm{diag}(\mathbf{z}_n)$ and $K = -\kappa(0)\,C\,\mathrm{diag}(\mathbf{y}_n)$. Hence, if C has complex eigenvalues (for example, in the case of symmetric or upwind discretiations), then the system {(2.1),(2.10c)} is only stable if $\kappa(0) = 0$. It should be remarked that application of the same integration method {(2.4), (2.5)} to different representations {**f**,**k**} will produce different numerical results. In this paper, we shall adjust the choice of a suitable representation to the iteration method used for solving the implicit relations in the integration method {(2.4), (2.5)} (see Section 3). ♦

In the following, we use the notation $\lambda(A)$ for the eigenvalues of a matrix A, $\delta(A)$ for $|\lambda(A)|_{min}$, and $\rho(A)$ for the spectral radius of A (from the context it will always be clear whether the Dahlquist polynomial $\rho$ or the spectral radius $\rho$ is meant). Furthermore, $\mathbb{S}$ will denote the stability region of the generating LMM.

## 3. Iterative solution of the implicit relations

If the LMM is a k-step method and if $\rho$ is normalized such that the coefficient of $E^k$ equals 1, then the equations to be solved in each step are given by

$$
\begin{aligned}
&\mathbf{y}_{n+k} - \alpha h\, \mathbf{f}(t_{n+k}, \mathbf{y}_{n+k}, \mathbf{z}_{n+k}) = (E^k - \rho(E))\mathbf{y}_n - h(\alpha E^k - \sigma(E))\, \mathbf{f}(t_n, \mathbf{y}_n, \mathbf{z}_n),\\
(3.1)\qquad &\mathbf{z}_{n+k} - \alpha h\, \mathbf{k}(t_{n+k}, t_{n+k}, \mathbf{y}_{n+k}, \mathbf{y}_{n+k}) = (E^k - \rho(E))\mathbf{z}_n - h\, \phi(t_{n+k},\mathbf{y}_{n+k}),\\
&\phi(t,\mathbf{y}) := (\alpha E^k - \sigma(E))\mathbf{k}(t, t_n, \mathbf{y}, \mathbf{y}_n),
\end{aligned}
$$

where $\alpha$ denotes the coefficient of $E^k$ in $\sigma$, to be assumed positive. Note that the equation for $\mathbf{z}_{n+k}$ becomes explicit if $\mathbf{k}(t, t, \mathbf{y}, \mathbf{y}) \equiv 0$. This happens in the PVIDEs (1.3), (1.4) and (1.5) if $\kappa(0) = 0$. In order to reduce the implicitness of the method (3.1), we shall replace the argument $\mathbf{y}_{n+k}$ in $\phi$ by the extrapolation $2\mathbf{y}_{n+k-1} - \mathbf{y}_{n+k-2}$.

Let us write the system (3.1) in the compact form

$$(3.2)\qquad \mathbf{R}(\mathbf{Y}_{n+k}) = \mathbf{0}, \quad \mathbf{Y}_{n+k} := \begin{pmatrix} \mathbf{y}_{n+k} \\ \mathbf{z}_{n+k} \end{pmatrix}.$$

Our starting point for solving (3.2) is the modified Newton method

$$(3.3)\qquad N\left(\mathbf{Y}^{(j)} - \mathbf{Y}^{(j-1)}\right) = -\mathbf{R}(\mathbf{Y}^{(j-1)}), \quad N := \begin{pmatrix} I - \alpha h \mathbf{f}_\mathbf{y} & -\alpha h \mathbf{f}_\mathbf{z} \\ -\alpha h(\mathbf{k}_\mathbf{y} + \mathbf{k}_\mathbf{w}) & I \end{pmatrix}.$$

In multi-dimensional problems, the solution of the linear sytems in (3.3) is quite expensive. In order to reduce these costs we shall replace the matrix N by a more 'convenient' matrix. Firstly, we shall ignore the matrices $\mathbf{f}_\mathbf{z}$ and $\mathbf{k}_\mathbf{y} + \mathbf{k}_\mathbf{w}$ in the iteration matrix N. Secondly, because of the considerable band width of the matrix $J = \mathbf{f}_\mathbf{y}$ in two- and three-dimensional problems, we shall approximate the matrix $I - \alpha hJ$ by an approximate factorization. Suppose that $J = J_1 + ... + J_d$, where d is the spatial dimension of (1.1) and where $J_i$ corresponds with the spatial derivative in the ith coordinate direction. Then, we can approximate the matrix $I - \alpha hJ$ by an approximate factorization based on the splitting $J = J_1 + ... + J_d$:

(3.4) $\Pi := \big(I - \alpha h J_1\big) \ldots \big(I - \alpha h J_d\big)$ .

If d = 1, then the approximation Π is of course exact. For $d \geq 2$, we have $\Pi = I - \alpha h J + O(h^2)$. For a detailed discussion of the approximation Π we refer to [7].

**Example 3.1.** We illustrate the splitting $J = J_1 + J_2$ for the population dynamics problem (1.3) on the 2-dimensional domain $\Omega = \{0 \leq x_1, x_2 \leq 1\}$ with homogeneous Dirichlet boundary conditions on the boundary of **Ω**. The Laplace operator Δ is replaced by a matrix D using standard symmetric differences on a grid with uniform gridsize Δx (compare Example 2.1). The functions **f** and **k** in (2.1) can be chosen e.g. according to

$$\mathbf{f}(t, \mathbf{y}, \mathbf{z}) = (D + bI)\mathbf{y} + \mathbf{yz} + \mathbf{g}(t), \quad \mathbf{k}(t, \tau, \mathbf{y}, \mathbf{w}) = -\,\kappa(t - \tau)\mathbf{w},$$

where I is the identity matrix, $\mathbf{g}(t)$ is the discrete analogue of $g(t,\mathbf{x})$ in (1.3). The Jacobian matrix $J = D + bI + \mathrm{diag}(\mathbf{z})$ can be split with $J_i = D_i + \frac{1}{2}(bI + \mathrm{diag}(\mathbf{z}))$, where $D_i$ represent the finite difference discretizations of $\partial^2/\partial x_i^2$. ♦

Approximations of the type (3.4) go back to Peaceman and Rachford [17] for solving elliptic and parabolic equations by the ADI method. The use of approximate factorization in iterative processes has been studied in [7, 9] for the solution of partial differential equations without quadrature terms. Here, we study the effect of including a quadrature term.
Thus, we consider the iterative method

(3.5) $\tilde{N}\big(\mathbf{Y}^{(j)} - \mathbf{Y}^{(j-1)}\big) = -\,\mathbf{R}(\mathbf{Y}^{(j-1)}), \quad \tilde{N} := \begin{pmatrix} \Pi & O \\ O & I \end{pmatrix}, \quad j = 1, \ldots, m,$

where $\mathbf{Y}^{(0)}$ is to be provided by a predictor formula. Each iteration consists of the solution of d linear systems with system matrix $I - \alpha h J_i$, i = 1, ... , d. However, these system matrices correspond with one-dimensional differential operators so that their band width is small (say less than 5). Hence, the LU decompositions and the forward-backward substitutions are not costly. Furthermore, in each iteration we need the evaluation of $\mathbf{f}(t_{n+k}, \mathbf{y}_{n+k}^{(j-1)}, \mathbf{z}_{n+k}^{(j-1)})$ and $\mathbf{k}(t_{n+k}, t_{n+k}, \mathbf{y}_{n+k}^{(j-1)}, \mathbf{y}_{n+k}^{(j-1)})$ and with each update of J, the LU decompositions of $I - \alpha h J_i$, i = 1, ... , d. Note that these function evaluations and LU decompositions can be done in parallel, which makes the algorithm suitable for implementation on a parallel computer system.
The form of the iteration method (3.5) strongly suggests choosing the representation {**f**, **k**} such that as much information on the problem as possible is contained in the Jacobian matrix $\mathbf{f_y}$, because in the approximation $\tilde{N}$ to the matrix N only the matrix $\mathbf{f_y}$ is taken into account. Thus, in Example 2.1 the representation (2.10c) is most appropriate, provided that κ(0) vanishes. Likewise, the matrix $\mathbf{f_y}$ corresponding with the representation given in Example 3.1 contains a maximal amount of information on the problem.

### 3.1. Convergence

The linearized recursion for the iteration error $\varepsilon^{(j)} := \mathbf{Y}^{(j)} - \mathbf{Y}_{n+k}$ associated with (3.5) is given by

$$\varepsilon^{(j)} = \big(I - \tilde{N}^{-1}N\big)\varepsilon^{(j-1)}, \quad I - \tilde{N}^{-1}N = \begin{pmatrix} I - \Pi^{-1}(I - \alpha hJ) & \alpha h\, \Pi^{-1}\mathbf{f_z} \\ \alpha h(\mathbf{k_y} + \mathbf{k_w}) & O \end{pmatrix}. \qquad (3.6)$$

As in the stability considerations in Section 2, we consider the model situation where the Jacobian matrices J, $\mathbf{f_z}$ and $\mathbf{k_y} + \mathbf{k_w}$ share the same eigensystems. Then, we find that the eigenvalues of the amplification matrix $I - \tilde{N}^{-1}N$ are given by those of the matrix

$$\begin{pmatrix} 1 - \lambda^{-1}(\Pi)\big(1 - \alpha h(\lambda(J))\big) & \alpha h\lambda^{-1}(\Pi)\lambda(\mathbf{f_z}) \\ \alpha h\lambda(\mathbf{k_y} + \mathbf{k_w}) & 0 \end{pmatrix}.$$

The iterative method (3.5) will be called *convergent* if these eigenvalues are within the unit circle. Writing

$$\xi := \lambda(J),\ \ \xi_k := \lambda(J_k),\ \ \eta := \lambda(K), \qquad (3.7)$$

where $K = \mathbf{f_z}(\mathbf{k_y} + \mathbf{k_w})$, and imposing the condition $|\lambda(I - \tilde{N}^{-1}N)| < 1$, will lead to a region in the $(h\xi_1, \ldots, h\xi_d, h^2\eta)$ - space. This region will be called the *region of convergence*.

**Theorem 3.1.** Let

$$P := (1 - \alpha h\xi_1) \ldots (1 - \alpha h\xi_d)\,,\ \ M := 1 - \alpha h\xi,\ \ T := P - M,\ \ \beta := \alpha^2h^2\eta. \qquad (3.8)$$

Then, the region of convergence is determined by the condition $|P|^2 - |\beta|^2 > |TP^* + \beta T^*|$, where $P^*$ and $T^*$ denote the complex conjugates to P and T.

**Proof.** The eigenvalues $\lambda(I - \tilde{N}^{-1}N)$ of the amplification matrix $I - \tilde{N}^{-1}N$ are the solutions of the characteristic equation $\lambda^2 - C_1\lambda - C_2 = 0$, where $C_1 = TP^{-1}$ and $C_2 = \beta P^{-1}$. Using Schur's criterion, we find that the region where $|\lambda(I - \tilde{N}^{-1}N)| < 1$ is determined by the inequalities $|C_2|^2 < 1$ and $|C_2|^2 < 1 - |C_1 + C_1^*C_2|$. Evidently, we may restrict our considerations to the second inequality. Since $|C_1 + C_1^*C_2| = |P|^{-2}\,|TP^* + \beta T^*|$, this inequality yields the convergence condition of the theorem.♦

We are particularly interested in the *stability region* of the iterated LMM. Obviously, this region is the intersection of the region of convergence and the region of stability of the LMM {(2.4), (2.5)}. The following three sections discuss stability regions in the case of one, two and three spatial dimensions.

### 3.2. One spatial dimension

Although we are mainly interested in the multidimensional case, we start with the one-dimensional case d = 1, where $\Pi = I - \alpha hJ$. This case shows us the largest stable stepsize that we are allowed to use on the basis of the test equation.

**Theorem 3.2.** The stability region of the iterated LMM {(2.4),(2.5)} contains the intersection of the stability region $\mathbb{S}$ of the LMM and the domain

(3.9) $$\{(h\xi, h^2\eta):\ \alpha|h^2\eta| < |h\xi - \alpha^{-1}|,\ \mathrm{Re}(\xi) \le 0,\ \ \mathrm{Im}(\eta) = 0\}.$$

**Proof.** If d = 1, then $P = 1 - \alpha h\xi$ and $T := 0$, so that by virtue of Theorem 3.1 the region of convergence $\mathbb{C}$ is determined by $\alpha|h^2\eta| < |h\xi - \alpha^{-1}|$. Since the stability region of the iterated LMM is the intersection of $\mathbb{C}$ and the region of stability $\mathbb{S}$ of the LMM, we find by virtue of Theorem 2.1 the result of the theorem.♦

In order to obtain stability conditions that can be used in practice, we derive the following corollaries.

**Corollary 3.1.** Let the eigenvalues $\xi$ and $\eta$ of J and K be real and let the underlying LMM be A-stable. Then, a necessary and sufficient condition for the stability of the iterated LMM is

(3.10) $$\xi \le 0,\ \ h < \frac{-\delta(J) + \sqrt{\delta^2(J) + 4\rho(K)}}{2\alpha\rho(K)}\ .$$

**Proof.** If $\xi$ is nonpositive and $\eta$ is real, then it follows from (3.9) that we have stability if $\alpha|\eta|h^2 + \xi h - \alpha^{-1} < 0$. This inequality is satisfied for all $\xi \le \delta(J)$ and all $|\eta| \le \rho(K)$ provided that $\alpha\rho(K)h^2 + \delta(J)h - \alpha^{-1} < 0$. This leads to the stepsize condition of the corollary.♦

**Corollary 3.2.** Let the eigenvalues $\xi$ and $\eta$ of J and K satisfy $\mathrm{Re}(\xi) \le 0$ and $\mathrm{Im}(\eta) = 0$, and let the underlying LMM be A-stable. Then, the following assertions hold for the iterated LMM:

(a) A sufficient condition for stability is

$$h^2 < \frac{\delta^2(J) + \sqrt{\delta^4(J) + 4\rho^2(K)}}{2\alpha^2\rho^2(K)}\ .$$

(b) Let h be the desired integration step. Then, a necessary and sufficient condition for stability is

$$\rho^2(K) < \alpha^{-4}h^{-4} + \alpha^{-2}h^{-3}\min_{\xi}\big(h|\xi|^2 - 2\alpha^{-1}\mathrm{Re}(\xi)\big).$$

**Proof.** We deduce from (3.9) that we have stability if

(3.11) $$\alpha^2\eta^2h^4 - |\xi|^2h^2 + 2\alpha^{-1}h\mathrm{Re}(\xi) - \alpha^{-2} < 0.$$

If $Re(\xi) \leq 0$, then this inequality is certainly satisfied if we ignore the term $2\alpha^{-1}hRe(\xi)$. The remaining inequalitiy is satisfied for all $\xi \leq \delta(J)$ and all $|\eta| \leq \rho(K)$ if we require that $\alpha^2\rho^2(K)h^4 - |\delta(J)|^2h^2 - \alpha^{-2} < 0$. This yields the stepsize condition given in part (a) of the corollary. Part (b) is immediate from (3.11).♦

**Example 3.2.** We illustrate Corollary 3.1 by means of Example 3.1 in the one-dimensional case (d = 1), where $J = D + bI + diag(\mathbf{z})$ and $K = -\kappa(0)\, diag(\mathbf{y})$. Let $y_i$ and $z_i$ denote the ith component of **y** and **z**, respectively. Then, the eigenvalues of K are given by $\lambda(K) = -\kappa(0)y_i$ and the eigenvalues of J satisfy the inequality $b - 4(\Delta x)^{-2} + z_{min} \leq \lambda(J) \leq b - \pi^2 + z_{max}$, where $z_{min} \leq z_i \leq z_{max}$. Hence, $\delta(J) = b - \pi^2 + z_{max}$ and $\rho(K) = |\kappa(0)|\, \|\mathbf{y}\|_\infty$. Thus, Corollary 3.1 leads to the conditions

$$b \leq \pi^2 - z_{max}, \quad h < \frac{\pi^2 - b - z_{max} + \sqrt{(\pi^2 - b - z_{max})^2 - 4|\kappa(0)|\,\|\mathbf{y}\|_\infty}}{2\alpha|\kappa(0)|\,\|\mathbf{y}\|_\infty} \; .♦$$

We conclude this section by plotting the domain (3.9) in the $(\alpha hRe(\xi), \alpha^2h^2Re(\eta))$ - plane and the $(\alpha hIm(\xi), \alpha^2h^2Re(\eta))$ - plane, respectively. The Figures 3.1 and 3.2 show these regions (black part corresponds with unstable points).

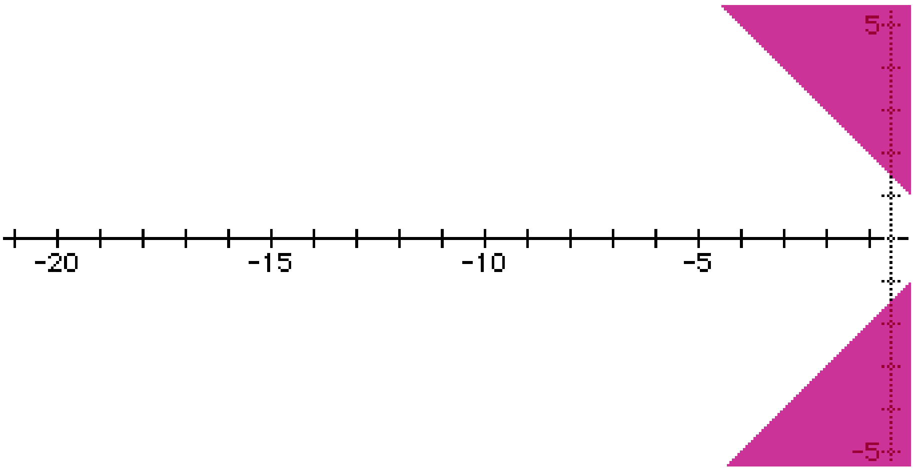


**Figure 3.1.** Stability region in the $(\alpha hRe(\xi), \alpha^2h^2Re(\eta))$ - plane.

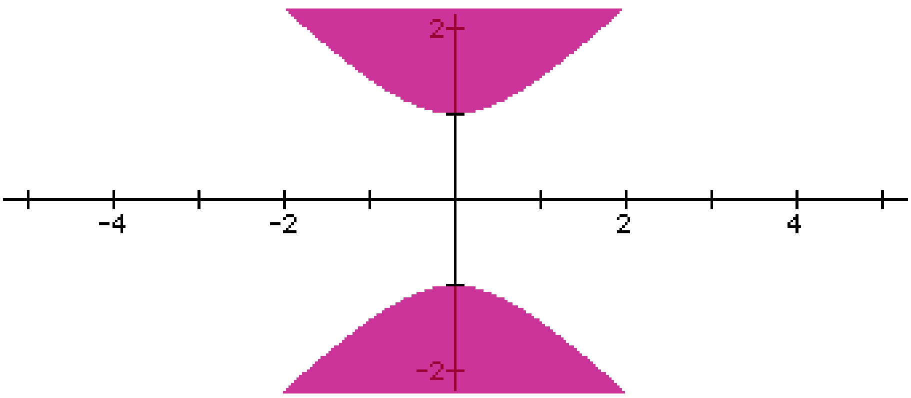


**Figure 3.2.** Stability region in the $(\alpha hIm(\xi), \alpha^2h^2Re(\eta))$ - plane.

### 3.3. Two spatial dimensions

For d = 2, the coefficient functions P and T in (3.8) are given by

(3.12) $$P := (1-\alpha h\xi_1)(1-\alpha h\xi_2), \quad T := \alpha^2 h^2 \xi_1 \xi_2.$$

**Theorem 3.3.** Let $a \le 0$ and let $\xi_1$, $\xi_2$ and $\eta$ be real. Then, the region of stability of the iterated LMM contains the intersection of $\mathbb{S}$ and the domain

$$\{(h\xi, h^2\eta):\ h\xi_1 \le a,\ h\xi_2 \le a,\ -(\alpha^{-1}-a)^2 < h^2\eta < \alpha^{-2} - 2a\alpha^{-1}\}.$$

**Proof.** If $h\xi_1 \le a$ and $h\xi_2 \le a$ with $a \le 0$, then we have in (3.12) $P > 0$ and $T > 0$, so that by virtue of Theorem 3.1 the region of convergence is determined by

$$(P - |\beta|)(P + |\beta|) > T\,|P + \beta|.$$

If $\eta \ge 0$, then $\beta \ge 0$, so that this condition reduces to $P - \beta > T$. From (3.12) it then follows that we should require $1 - \alpha h\xi > \beta = \alpha^2 h^2 \eta$, i.e. $\alpha^2 h^2 \eta < 1 - 2a\alpha$. If $\eta \le 0$, then $\beta \le 0$, so that we have $(P+\beta)(P-\beta) > T\,|P+\beta|$. If $P + \beta < 0$, then $P - \beta < -T$, which is impossible. Hence, we assume $P + \beta > 0$, leading to $1 - \alpha h\xi > \beta$. The inequality $P + \beta > 0$ is equivalent with $\alpha^2 h^2 \eta > -(1-\alpha h\xi_1)(1-\alpha h\xi_2)$, which is satisfied if $\alpha^2 h^2\eta > -(1-a\alpha)^2$, and the inequality $1 - \alpha h\xi > \beta$ is equivalent with $\alpha^2 h^2 \eta < 1 - \alpha h\xi$, which is always satisfied for $\eta \le 0$. Thus, the convergence region is determined by $h\xi_1 \le a$, $h\xi_2 \le a$ and $-(\alpha^{-1}-a)^2 < h^2\eta < \alpha^{-2} - 2a\alpha^{-1}$. Taking the intersection with $\mathbb{S}$ (see Theorem 2.1), we obtain the stability region as given by the theorem. ♦

**Corollary 3.3.** Let the eigenvalues $\xi_1$ and $\xi_2$ of $J_1$ and $J_2$ be real and nonpositive, let the eigenvalues $\eta$ of K be real, and define

$$\xi_0 := \min\{\delta(J_1), \delta(J_2)\}, \quad \eta_0 := \xi_0 + \max_{\eta \le -\xi_0^2} \sqrt{-\eta}, \quad \eta_1 := \max_{\eta \ge 0} \eta,$$

where $\eta_0 = 0$ if $\lambda(K) \ge -\xi_0^2$ and $\eta_1 = 0$ if all $\lambda(K) \le 0$. Then the iterated LMM {(2.4), (2.5)} is stable if the underlying LMM is A-stable and if

$$h < \min\left\{\frac{1}{\alpha\eta_0}, \frac{-\xi_0 + \sqrt{\xi_0^2 + \eta_1}}{\alpha\eta_1}\right\}.$$

**Proof.** Applying Theorem 3.3 with $\xi_1 \le \xi_0$, $\xi_2 \le \xi_0$, and $a = h\xi_0$, we find that we have stability if

$$h < \frac{1}{\alpha(\xi_0 + \sqrt{-\eta})} \ \text{ for } \eta \le -\xi_0^2, \quad h < \frac{-\xi_0 + \sqrt{\xi_0^2 + \eta}}{\alpha\eta} \ \text{ for } \eta \ge 0.$$

The right-hand sides in the inequalities are monotonically decreasing with $|\eta|$, proving the corollary. ♦

Thus, we have unconditional stability if $J_1$ and $J_2$ have negative eigenvalues $\le \xi_0$ and if K has eigenvalues in $[-\xi_0^2, 0]$. This is surprising, because in the one-dimensional case, where approximate factorization is not needed, we do not have a region of unconditional stability (see Corollary 3.1).

**Example 3.3.** We illustrate this Corollary 3.3 by means of Example 3.1 with d = 2 and the splitting $J_1 = D_1 + \frac{1}{2}\big(bI + \mathrm{diag}(\mathbf{z})\big)$ and $J_2 = D_2 + \frac{1}{2}\big(bI + \mathrm{diag}(\mathbf{z})\big)$, so that $\delta(J_1) = \delta(J_2) = \frac{1}{2}(b - 2\pi^2 + z_{max})$ and $\lambda(K) = -\kappa(0)y_i$. Assuming that $\kappa(0) \ge 0$ and $b \le 2\pi^2 - z_{max}$, and because $y_i > 0$ (recall that $y_i$ represents the size of the population), we have

$$\xi_0 = \frac{1}{2}(b - 2\pi^2 + z_{max}), \quad \eta_0 = \max_{y_i \ge y_0} \sqrt{\kappa(0)y_i} + \frac{1}{2}(b - 2\pi^2 + z_{max}),$$

$$\eta_1 = 0, \quad y_0 := \frac{(2\pi^2 - b - z_{max})^2}{4\kappa(0)},$$

where $\eta_0 = 0$ if all $y_i \le y_0$. Hence, if all $y_i \le y_0$, then we have unconditional stability and if one or more $y_i > y_0$, then we should satisfy the stepsize condition

$$h < \frac{2}{\alpha\left(2 \max_{y_i \ge y_0} \sqrt{\kappa(0)y_i} + b - 2\pi^2 + z_{max}\right)}. \blacklozenge$$

**Theorem 3.4.** Let $\xi_1$ and $\xi_2$ be complex and let $\eta$ be real. Then, the region of stability of the iterated LMM contains the intersection of $\mathbb{S}$ and the domain

$$\{(h\xi_1, h\xi_2, h^2\eta):\ \mathrm{Re}(\xi_1) \le 0,\ \mathrm{Re}(\xi_2) \le 0,\ -\alpha^{-2} < h^2\eta < \alpha^{-2}\}.$$

**Proof.** Let us consider the most critical case where $\xi_1$ and $\xi_2$ are purely imaginary, so that in (3.12) $T \le 0$, so that by virtue of Theorem 3.1 the region of convergence is determined by

$$|P|^2 - |\beta|^2 > -T|P^* + \beta|.$$

We verify this inequality for $-\alpha^{-2} < h^2\eta < \alpha^{-2}$, i.e. $-1 < \beta < 1$. Let us write $h\xi_1 = ix_1$, $h\xi_2 = ix_2$, and $h^2\eta = x$. Then this inequality becomes

$$\alpha^4x^2 < (1 + \alpha^2x_1^2)(1 + \alpha^2x_2^2) - \alpha^2|x_1x_2|\sqrt{\big(1 - \alpha^2(x_1x_2 - x)\big)^2 + \alpha^2\big(x_1 + x_2\big)^2}. \tag{3.13}$$

On substitution of $\beta = \pm 1$, i.e. $x = \pm\alpha^{-2}$, we obtain

$$(\alpha^2x_1^2x_2^2 + (x_1 - x_2)^2)(x_1 + x_2)^2 > 0, \quad x_1^4 + x_2^4 + \alpha^2x_1^2x_2^2(x_1 - x_2)^2 + 2x_1^2x_2^2 > 0.$$

These inequalities are clearly satisfied for all $x_1 \ne 0$ and $x_2 \ne 0$, yielding the result of the theorem. ♦

For $\alpha^4x^2 > 0$, the region $\mathbb{C}$ in the $(x_1,x_2)$-plane satisfying (3.13) is bounded. We illustrate this for $\alpha = 2/3$ and $x = \pm 5$. Figures 3.3 and 3.4 present $\mathbb{C}$ for $x = 5$ and $x = -5$, respectively (the black part represent points of divergence).

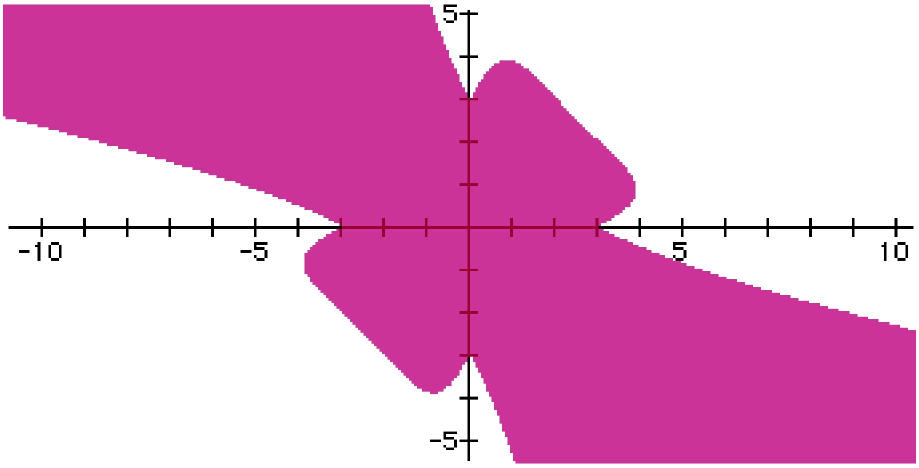


**Figure 3.3.** Region in the $(\mathrm{Im}(h\xi_1), \mathrm{Im}(h\xi_2))$ - plane satisfying (3.13) for $h^2\eta = 5$.

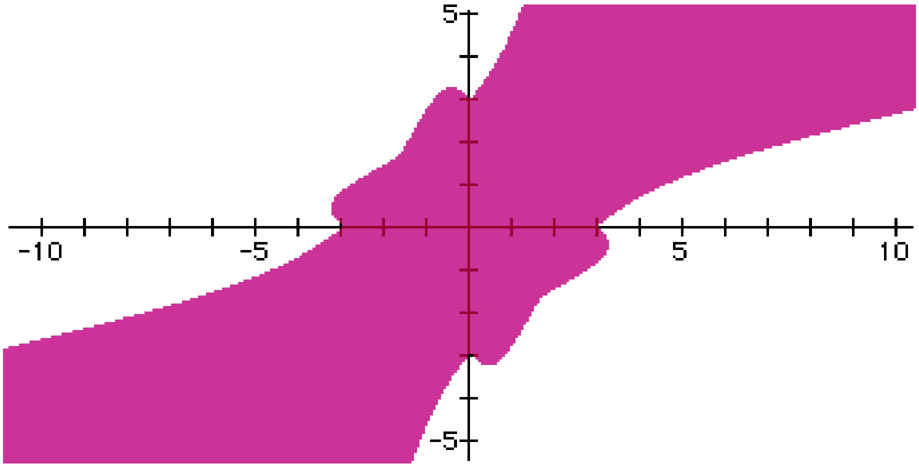


**Figure 3.4.** Region in the $(\mathrm{Im}(h\xi_1), \mathrm{Im}(h\xi_2))$ - plane satisfying (3.13) for $h^2\eta = -5$.

We verified that for $x \geq 0$ and $x \leq 0$ the value of $|\lambda(I - \tilde{N}^{-1}N)|$ increases most rapidly along the lines $x_1 = -x_2$ and $x_1 = x_2$, respectively. Hence, taking $x_1 = -x_2$ if $x \geq 0$ and $x_1 = x_2$ if $x \leq 0$, we can plot in the $(x_1, x)$ - plane a domain which is contained in the convergence region (see Figure 3.5).

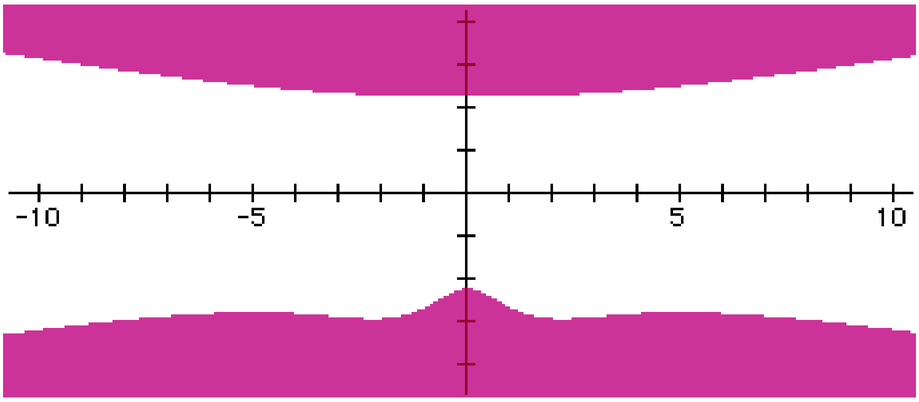


**Figure 3.5.** Region of convergence in the $(\mathrm{Im}(h\xi_1), h^2\eta)$ - plane.

**3.4. Three spatial dimensions**

Suppose that in Theorem 3.1 the parameter $\beta$ vanishes. Then, the region of convergence is determined by the inequality $|P| > |T|$. Inequalities of this type have been studied in [7]. For three spatial dimensions (d = 3) it was found that the convergence region contains the region $\{(h\xi_1, h\xi_2, h\xi_3): |\arg(-\xi_j)| \le \pi/4, j = 1, 2, 3\}$. This result leads us to set $\alpha h\xi_1 = x\exp(i\theta)$, $\alpha h\xi_2 = y\exp(i\theta)$, $\alpha h\xi_3 = z\exp(i\theta)$, where either $\theta = 3\pi/4$ or $\theta = 5\pi/4$, and to consider the range of (real) $\beta$-values for which the convergence condition

$$Q(x,y,z,\beta) := (|P(\theta)|^2 - \beta^2)^2 - |T(\theta)P^*(\theta) + \beta T^*(\theta)|^2 > 0$$

in Theorem 3.1 is satisfied for all nonnegative x, y and z values. Since $P(3\pi/4) = P^*(5\pi/4)$ and $T(3\pi/4) = T^*(5\pi/4)$, the function Q does not depend on $\theta$. Using Maple, we found that $Q(x,y,z,\beta)$ can be expressed in the form

$$\begin{aligned} Q = \; & \big[(\beta_0 z^2 + 2z + \beta_0)y^3 + (\beta_0 z^3 + 5z^2 + 4\beta_0 z + 3)y^2 + (2z^3 + 4\beta_0 z^2 + 6z + 2\beta_0)y \\ & + \beta_0 z^3 + 3z^2 + 2\beta_0 z + 1\big]\, x^4 + \\ & \big[(\beta_0 z^2 + 2z + \beta_0)y^4 + (\beta_2 z^3 + \beta_1 z^2 + \beta_3 z + 6)y^3 + (\beta_0 z^4 + \beta_1 z^3 + \beta_4 z^2 + \beta_5 z \\ & + \beta_6)y^2 + (2z^4 + \beta_3 z^3 + \beta_5 z^2 + \beta_7 z + 8)y + \beta_0 z^4 + 6z^3 + \beta_6 z^2 + 8z + 2\beta_0\big]x^3 + \\ & \big[(\beta_0 z^3 + 5z^2 + 4\beta_0 z + 3)y^4 + (\beta_0 z^4 + \beta_1 z^3 + \beta_4 z^2 + \beta_5 z + \beta_6)y^3 + (5z^4 + \beta_4 z^3 \\ & + \beta_8 z^2 + \beta_9 z + \beta_{10})y^2 + (4\beta_0 z^4 + \beta_5 z^3 + \beta_9 z^2 + \beta_{11} z + \beta_{12})y + 3z^4 + \beta_6 z^3 \\ & + \beta_{10} z^2 + \beta_{12} z + \beta_{13}\big]\, x^2 + \\ & \big[(2z^3 + 4\beta_0 z^2 + 6z + 2\beta_0)y^4 + (2z^4 + \beta_3 z^3 + \beta_5 z^2 + \beta_7 z + 8)y^3 + (4\beta_0 z^4 + \beta_5 z^3 \\ & + \beta_9 z^2 + \beta_{11} z + \beta_{12})y^2 + (6z^4 + \beta_7 z^3 + \beta_{11} z^2 + \beta_{14} z + \beta_{15})y + 2\beta_0 z^4 + 8z^3 \\ & + \beta_{12} z^2 + \beta_{15} z + \beta_{16}\big]\, x + \\ & \big[(\beta_0 z^3 + 3z^2 + 2\beta_0 z + 1)y^4 + (\beta_0 z^4 + 6z^3 + \beta_6 z^2 + 8z + 2\beta_0)y^3 \\ & + (3z^4 + \beta_6 z^3 + \beta_{10} z^2 + \beta_{12} z + \beta_{13})y^2 + (2\beta_0 z^4 + 8z^3 + \beta_{12} z^2 + \beta_{15} z + \beta_{16})y \\ & + (z^4 + 2\beta_0 z^3 + \beta_{13} z^2 + \beta_{16} z + \beta_{17})\big], \end{aligned}$$

where

$$\begin{array}{lll} \beta_0 = 2\sqrt{2}, & \beta_1 = 10 + 2\beta, & \beta_2 = (2 + \beta)\beta_0, \\ \beta_3 = (8 + \beta)\beta_0, & \beta_4 = (16 + 3\beta)\beta_0, & \beta_5 = 22 + 4\beta, \\ \beta_6 = (7 + \beta)\beta_0, & \beta_7 = (14 + 2\beta)\beta_0, & \beta_8 = 42 + 12\beta - 3\beta^2, \\ \beta_9 = (26 + 7\beta - 3\beta^2)\beta_0, & \beta_{10} = 15 - 3\beta^2 + 2\beta, & \beta_{11} = 30 - 6\beta^2 + 4\beta, \\ \beta_{12} = (8 - 2\beta^2)\beta_0, & \beta_{13} = 4 - 2\beta^2, & \beta_{14} = (16 - 4\beta^2)\beta_0, \\ \beta_{15} = 8 - 4\beta^2, & \beta_{16} = (2 - 2\beta^2)\beta_0, & \beta_{17} = (1 - \beta^2)^2. \end{array}$$

If $|\beta| < 1$, then all coefficients $\beta_j$ are positive, so that Q is positive for all nonnegative values of x, y and z. Hence, we have proved:

**Theorem 3.5.** Let $\xi_1$, $\xi_2$ and $\xi_3$ be complex and let $\eta$ be real. Then, the region of stability of the iterated LMM contains the intersection of $\mathbb{S}$ and the domain

$$\{(h\xi_1, h\xi_2, h\xi_3, h^2\eta): \; |\arg(-\xi_j)| \le \pi/4, \; j = 1, 2, 3, \;\; -\alpha^{-2} < h^2\eta < \alpha^{-2}\}. \; \blacklozenge$$

## 4. Numerical experiments

In our numerical experiments, we used the L-stable, second-order backward differentiation formula (BDF) and the A-stable, second-order trapezoidal rule (TR) for integrating $\mathbf{y}' = \mathbf{f}(t, \mathbf{y}, \mathbf{z})$. This respectively yields the formulas

(4.1a) $$\mathbf{y}_{n+1} = \tfrac{4}{3}\mathbf{y}_n - \tfrac{1}{3}\mathbf{y}_{n-1} + \tfrac{2}{3} h\, \mathbf{f}(t_{n+1}, \mathbf{y}_{n+1}, \mathbf{z}_{n+1}), \quad n = 1, 2, ...,$$

(4.2a) $$\mathbf{y}_{n+1} = \mathbf{y}_n + \tfrac{1}{2} h \Big(\mathbf{f}(t_n, \mathbf{y}_n, \mathbf{z}_n) + \mathbf{f}(t_{n+1}, \mathbf{y}_{n+1}, \mathbf{z}_{n+1})\Big), \quad n = 0, 1, ...,$$

where $\mathbf{z}_{n+1} = \mathbf{z}(t_{n+1}, t_{n+1})$ is obtained from a numerical integration of (2.3). In both cases (4.1a) and (4.2a) we again used the second-order BDF and the TR, respectively. The starting value needed by the BDF was computed by backward Euler.
In order to reduce the degree of implicitness, we replace in the first n steps of the integration of (2.3) the value of $\mathbf{y}_{n+1}$ by the extrapolation $2\mathbf{y}_n - \mathbf{y}_{n-1}$. Thus, in the BDF case

(4.1b) $$\mathbf{z}_{\nu+1} = \tfrac{4}{3}\mathbf{z}_\nu - \tfrac{1}{3}\mathbf{z}_{\nu-1} + \tfrac{2}{3} h\, \mathbf{k}(t_{n+1}, t_{\nu+1}, 2\mathbf{y}_n - \mathbf{y}_{n-1}, \mathbf{y}_{\nu+1}), \quad \nu \le n-1,$$

(4.1c) $$\mathbf{z}_{n+1} = \tfrac{4}{3}\mathbf{z}_n - \tfrac{1}{3}\mathbf{z}_{n-1} + \tfrac{2}{3} h\, \mathbf{k}(t_{n+1}, t_{n+1}, \mathbf{y}_{n+1}, \mathbf{y}_{n+1}),$$

and in the TR case

(4.2b) $$\mathbf{z}_{\nu+1} = \mathbf{z}_\nu + \tfrac{1}{2} h\Big(\mathbf{k}(t_{n+1}, t_\nu, 2\mathbf{y}_n - \mathbf{y}_{n-1}, \mathbf{y}_\nu) + \mathbf{k}(t_{n+1}, t_{\nu+1}, 2\mathbf{y}_n - \mathbf{y}_{n-1}, \mathbf{y}_{\nu+1})\Big),$$

(4.2c) $$\mathbf{z}_{n+1} = \mathbf{z}_n + \tfrac{1}{2} h\Big(\mathbf{k}(t_{n+1}, t_n, 2\mathbf{y}_n - \mathbf{y}_{n-1}, \mathbf{y}_n) + \mathbf{k}(t_{n+1}, t_{n+1}, \mathbf{y}_{n+1}, \mathbf{y}_{n+1})\Big),$$

where $\nu \le n - 1$. The extrapolation of $\mathbf{y}_{n+1}$ does not affect the accuracy or the stability, so that the methods (4.1) and (4.2) are both second-order accurate and their stability region with respect to the test equation (2.6) still contains the domains (2.9a) and (2.9b).
We illustrate the performance of the iterated BDF and TR by integrating the population dynamics problems (1.3) and (1.5). Both problems were discretized on the two-dimensional domain $\Omega = \{0 \le x_1 \le 1, 0 \le x_2 \le 1\}$ with homogeneous Dirichlet boundary conditions using second-order symmetric finite differences on a uniform, cartesian grid with meshsize $\Delta x$. We prescribed the exact solution $u(t,\mathbf{x})$ by

(4.3) $$u(t,\mathbf{x}) = e^{-t}\, x_1 x_2 (1 - x_1)(1 - x_2)$$

and determined the function $g(t,\mathbf{x})$ accordingly.

In order to clearly see the algorithmic properties of the approximate factorization approach, we used a fixed stepsize h and a fixed number of iterations m. For the initial approximation to the solution ($\mathbf{y}_{n+1}$, $\mathbf{z}_{n+1}$) of (4.1) and (4.2) we simply used ($\mathbf{y}_n$, $\mathbf{z}_n$). The maximal absolute errors produced at the end point were written as $10^{-cd}$, so that cd can be interpreted as the number of correct digits.

### 4.1. Diffusion model

In the diffusion model (1.3), we chose

(4.4) $\kappa(t) = e^{-t}$, $b = 1$, $0 \le t \le 2$.

The functions **f** and **k** were chosen as in Example 3.1. In order to avoid updates of LU decompositions, we approximated the matrix $J = \mathbf{f}_\mathbf{y} = D + I + \mathrm{diag}(\mathbf{z})$ by the constant matrix D + I. The Jacobian splitting was also chosen as in Example 3.1. The Tables 4.1 and 4.2 list the cd-values obtained by the BDF and the TR for $\Delta x_1 = \Delta x_2 = 1/40$ and for a few h and m. From these results we see that (i) the second-order behaviour is shown, (ii) the methods remain stable for relatively large stepsizes, (iii) the number of iterations needed to solve the implicit relations varies from 3 for small to 5 for large stepsizes, and (iv) TR is slightly more accurate than BDF because of its smaller error constant.

**Table 4.1.** cd-values of BDF for problem {(1.3),(4.3),(4.4)}.

| h | m = 1 | m = 2 | m = 3 | m = 5 | … | m = 10 |
|---|---|---|---|---|---|---|
| 1/5 | 2.9 | 3.6 | 4.2 | 5.1 | … | 5.1 |
| 1/10 | 3.5 | 4.5 | 5.5 | 5.8 | … | 5.8 |
| 1/20 | 4.2 | 5.6 | 6.5 | 6.4 | … | 6.4 |
| 1/40 | 4.8 | 6.7 | 7.0 | 7.0 | … | 7.0 |
| 1/80 | 5.4 | 7.6 | 7.6 | 7.6 | … | 7.6 |

**Table 4.2.** cd-values of TR for problem {(1.3),(4.3),(4.4)}.

| h | m = 1 | m = 2 | m = 3 | m = 5 | … | m = 10 |
|---|---|---|---|---|---|---|
| 1/5 | 3.4 | 4.2 | 4.9 | 5.8 | … | 5.8 |
| 1/10 | 4.0 | 5.1 | 6.1 | 6.5 | … | 6.4 |
| 1/20 | 4.6 | 6.2 | 7.0 | 7.0 | … | 7.0 |
| 1/40 | 5.2 | 7.2 | 7.6 | 7.6 | … | 7.6 |
| 1/80 | 5.8 | 8.2 | 8.2 | 8.2 | … | 8.2 |

### 4.2. Diffusion-convection model

In the diffusion-convection model (1.5), we chose

(4.5) $\kappa(t) = t\, e^{-t}$, $\mathbf{v} = (1,2)^T$, $0 \le t \le 1$

and we defined the functions **f** and **k** according to (2.10c). Note that with this representation we do not need boundary conditions for **z**, because **y** satisfies homogeneous boundary conditions. The matrix J is given by J = D + C diag($\mathbf{z}_n$). Again, in order to avoid updates of LU decompositions, we approximated J by the matrix D. The Jacobian splitting was defined according to dimension splitting. Unlike the discretization of the diffusion model {(1.3),(4.3),(4.4)}, the spatial error of the discretization of the diffusion-convection model {(1.5),(4.3),(4.5)} does not vanish. Therefore, we present results on a relatively fine mesh with $\Delta x_1 = \Delta x_2 = 1/80$, so that the temporal error is dominating. The Tables 4.3 and 4.4 list the results obtained by the BDF and TR methods. We see a similar behaviour as for problem {(1.3),(4.3),(4.4)}. For stepsizes h ≤ 1/80, the spatial error becomes dominant, so that the cd-values start to converge to a constant value.

**Table 4.3.** cd-values of BDF for problem {(1.5),(4.3),(4.5)}.

| h | m = 1 | m = 2 | m = 3 | m = 5 | … | m = 10 |
|---|---|---|---|---|---|---|
| 1/5 | 2.4 | 3.1 | 3.7 | 4.6 | … | 4.6 |
| 1/10 | 3.1 | 4.0 | 5.0 | 5.4 | … | 5.3 |
| 1/20 | 3.7 | 5.1 | 6.0 | 6.0 | … | 5.9 |
| 1/40 | 4.3 | 6.2 | 6.6 | 6.5 | … | 6.5 |
| 1/80 | 4.9 | 7.1 | 7.0 | 7.0 | … | 7.0 |
| 1/160 | 5.5 | 7.4 | 7.3 | 7.3 | … | 7.3 |

**Table 4.4.** cd-values of TR for problem {(1.5),(4.3),(4.5)}.

| h | m = 1 | m = 2 | m = 3 | m = 5 | … | m = 10 |
|---|---|---|---|---|---|---|
| 1/5 | 2.9 | 3.7 | 4.4 | 5.2 | … | 5.4 |
| 1/10 | 3.5 | 4.6 | 5.6 | 6.0 | … | 6.0 |
| 1/20 | 4.1 | 5.7 | 6.5 | 6.6 | … | 6.6 |
| 1/40 | 4.8 | 6.7 | 7.1 | 7.1 | … | 7.1 |
| 1/80 | 5.4 | 7.5 | 7.4 | 7.4 | … | 7.4 |
| 1/160 | 6.0 | 7.5 | 7.4 | 7.4 | … | 7.4 |

**References**

[1] A. Belleni-Morante, An integro-differential equation arising from the theory of heat conduction in rigid materials with memory, Boll. Un. Mat. Ital. B (5), 15 (1978), 470-482.

[2] H. Brunner and P.J. van der Houwen, The Numerical Solution of Volterra Equations, CWI Monographs, Vol. 3, North-Holland, Amsterdam, 1986.

[3] H. Brunner and J.D. Lambert, Stability of numerical methods for Volterra integro-differential equations, Computing, 12 (1974), 75-89.

[4] C. Chen and T. Shih, Finite Element Methods for Integrodifferential Equations, Series on Applied Math., Vol. 9, World Scientific, Singapore, 1998.

[5] J.M. Cushing, Integro-Differential Equations and Delay Models in Population Dynamics, Lecture Notes Biomath., Vol. 20, Springer-Verlag, New York, 1977.

[6] C.M. Dafermos and J.A. Nohel, A nonlinear hyperbolic Volterra equation in viscoelasticity, in: Contributions to Analysis and Geometry (Eds. D.N. Clark, G. Pecelli, R. Sacksteder), Supplement to American J. Math. (1981), 87-116.

[7] C. Eichler-Liebenow, P.J. van der Houwen and B.P. Sommeijer, Analysis of approximate factorization in iteration methods, Appl. Numer. Math., 28 (1998), 245-258.

[8] P.J. van der Houwen and B.P. Sommeijer, Euler-Chebyshev methods for integro-differential equations, Appl. Numer. Math., 24 (1997), 203-218.

[9] P.J. van der Houwen and B.P. Sommeijer, The use of approximate factorization methods in stiff ODE solvers, J. Comput. Appl. Math. 100 (1998), 11-21.

[10] M. Iida, Exponentially asymptotic stability for a certain class of semilinear Volterra diffusion equations, Osaka Math. J., 28 (1991), 411-440.

[11] T. Ikeda, Stationary solutions of a spatially aggregating population model, Proc. Japan Acad. Ser. A. Math. Sci., 60 (1984), 46-48.

[12] J. Matthys, A-stable linear multistep methods for Volterra integro-differential equations, Numer. Math., 27 (1976), 85-94.

[13] M. Mimura, Some convection-diffusion equations arising in population dynamics, in: Nonlinear Partial Differential Equations, Durham, N.H., 1982, pp. 343-351, Contemp. Math., Vol. 17, Amer. Math. Soc., Providence, RI, 1983.

[14] M. Mimura and K. Ohara, Standing wave solutions for a Fisher type equation with nonlocal convection, Hiroshima Math. J., 16 (1986), 33-50.

[15] M. Mimura and S. Takigawa, A size-distribution model with density-dependent growth rates, Japan J. Appl. Math., 5 (1988), 33-51.

[16] T. Nagai, Some nonlinear degenerate diffusion equations related to population dynamics, J. Math. Soc. Japan, 35 (1983), 539-562.

[17] D.W. Peaceman and H.H. Rachford Jnr., The numerical solution of parabolic and elliptic differential equations, J. Soc. Indust. App. Math. 3 (1955), 28-41.

[18] J. Prüss, Evolutionary Integral Equations and Applications, Birkhäuser Verlag, Basel, 1993. [See especially pp. xii-xv, Ch. 5 (parabolic VIDEs), Ch. 9 (hyperbolic VIDEs), Ch. 13, and the extensive bibliography.]

[19] S. Shaw and J.R. Whiteman, Towards adaptive finite element schemes for partial differential Volterra equation solvers, Advances Comput. Math., 6 (1996), 309-323.

[20] A.S. Vasudeva Murthy and J.G. Verwer, Solving parabolic integro-differential equations by an explicit integration method, J. Comput. Appl. Math., 39 (1992), 121-132.

[21] V. Volterra, Sulle equazioni integro-differenziali, Rend. Accad. Lincei (5), 18 (1909), 167-174.

[22] Y. Yamada, On a certain class of semilinear Volterra diffusion equations, J. Math. Anal. Appl., 88 (1982), 433-451.

[23] Y. Yamada, On some semilinear Volterra diffusion equations arising in ecology, in: Equadiff 5 (Bratislava, 1981), pp. 370-373, Teubner, Leipzig, 1982.

[24] E.G. Yanik and G. Fairweather, Finite element methods for parabolic and hyperbolic partial integro-differential equations, Nonlinear Anal., 12 (1988), 785-809.

[25] N.-Y. Zhang, On the Discretization in Time and Space of Partial Integro-Differential Equations, Doctoral Thesis, Dept. of Mathematics, Chalmers University of Technology, Göteborg, 1990.